23

Rotation angle sensor based on a one-dimensional photonic crystal with a defect

© A.I. Sidorov[1,2], A.A. Efimov[2]

[1] ITMO University,
197101 St. Petersburg, Russia
[2] St. Petersburg State Electrotechnical University „LETI“,
197376 St. Petersburg, Russia

e-mail: sidorov@oi.ifmo.ru

Received January 26, 2023
Revised January 26, 2023
Accepted April 20, 2023

The results of numerical simulation of the optical properties of a one-dimensional (1D) photonic crystal with a defect based on semiconductor-dielectric layers in the near-IR range are presented. The simulations used layers of silicon and silicon dioxide with optical thicknesses $3\lambda/4$, $\lambda/4$ and $10\lambda/4$. The influence of radiation incident angle on the spectral position of the defect's guidance band has been studied. It is shown that the sensitivity to the rotation angle lies within the limits of 6−20 nm/deg and 1.7−5.5 dB/deg, depending on the geometry of the sensor and the measurement method. This makes these photonic crystals promising for use in the rotation angle sensors as a sensitive element.

Keywords: rotation angle sensor, incident angle, photonic crystal, photonic band gap, transfer matrix.

DOI: 10.61011/EOS.2023.07.57144.4568-23

Introduction

Rotation angle sensors are widely used in industry, monitoring of structures and buildings, transport, robotics and other areas of human activity. Currently, there is a huge number of angle sensors based on various physical processes [1]. Most of them are based on mechanical, electrical, magnetic and optical effects [2–7]. Rotation angle sensors can also be used to detect displacement, bend and twist angles. Optical angle sensors provide high resolution. They have high sensitivity and are not sensitive to electromagnetic blasts.

Photonic crystals and photonic crystal fibers are widely used in sensing [8–14]. They are used to measure temperature, medium refraction index, electric and magnetic fields, mechanical stress, angles, etc. Photonic crystals and fibers are resonance optical systems. Their spectral and amplitude characteristics depend on external and internal changes, such as temperature, pressure, field-induced birefringence, and medium refraction index. All these effects can be used in the development of sensors. For example, as shown in [15], the coupling strength between the internal resonance optical modes of a photonic crystal depends on the radiation incident angle. This can be used to measure the incident angle by measuring the intensity of transmitted radiation. When using high Q-factor modes, the sensitivity of such a device can reach its maximum.

If the periodicity of the photonic crystal is disrupted by a defect, then a specific spectral area with different optical properties can be created. The defect area can support modes with frequencies inside the photonic band gap. But since the defect guidance band is surrounded by a photonic band gap, emission within the defect remains limited. As a rule, the defect guidance band is very narrow. This allows the creation of sensors with very high sensitivity.

The aim of this paper was to study the optical properties of a 1D photonic crystal with a defect from the point of view of the opportunity of its use as a rotation angle sensor, as well as to consider the influence of the geometry of the photonic crystal on its angular sensitivity.

Photonic crystal geometry and numerical simulation technique

A 1D photonic crystal consists of 4 pairs of $Si-SiO_2$ layers with a SiO_2 defect in the center (Fig. 1). Si and SiO_2 layers have a high refraction index contrast: 3.4 and 1.46 accordingly. This allows the use of only 4 pairs of layers in a photonic crystal without deteriorating its optical characteristics. The layers can be formed by vacuum deposition on silicon wafers with a thickness of 1−2 mm. The top silicon wafer can be coupled to the photonic crystal using an immersion layer. The outer surfaces of silicon wafers should have anti-reflective coatings. It should be noted that the internal surfaces of silicon wafers participate in interference processes in a photonic crystal. Two photonic crystal geometries were used in the numerical simulation. In the first geometry, the optical thickness of the layers was equal to $\lambda/4$ for $\lambda = 1.5\,\mu$m. For Si layers this is $0.118\,\mu$m and for SiO layers $_2$ — $0.274\,\mu$m. The thickness of the defect layer is $0.7\,\mu$m. In the second geometry, the optical

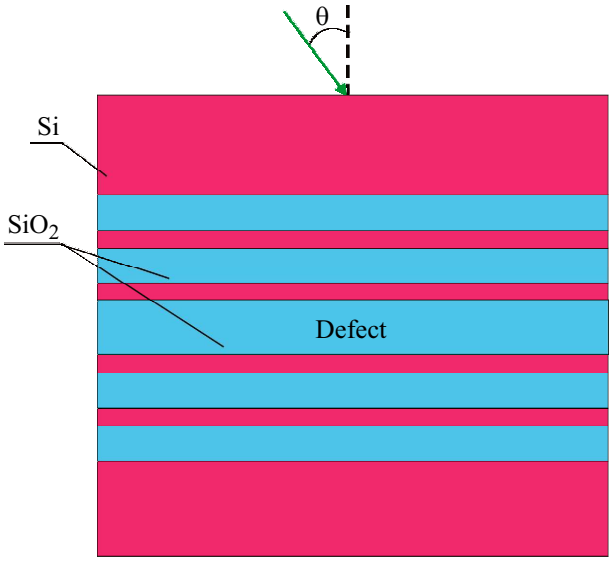

Figure 1. Geometry of a 1D photonic crystal with a defect.

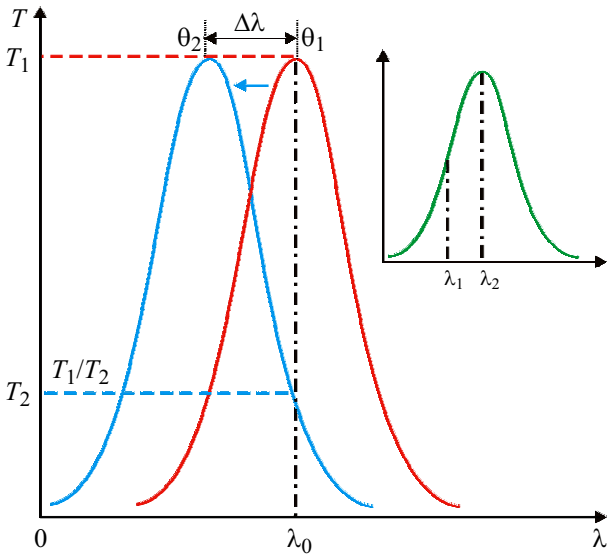

Figure 2. Two methods for measuring the incident angle (the explanations are given in the text).

thickness of the layers was equal to $10\lambda/4$, and the thickness of the defect layer was — $7\,\mu$m.

Fig. 2 presents two methods for measuring the incident angle θ. Since a change in the incident angle leads to a spectral shift in the guidance band of a photonic crystal defect, the spectral shift $\Delta\lambda$ of the defect guidance band can be used to determine the change in the incident angle. For these purposes a spectrophotometer can be used. However, to increase the sensitivity and to reduce the dimensions of the sensor measuring part, it is preferable to use a narrow-band tunable semiconductor DFB laser as a radiation source. In this case a photodiode can be used as a photodetector. The second method is based on measuring the transmittance of a photonic crystal at a fixed wavelength λ_0 corresponding to the wavelength of the probing laser. However, in this case, uncertainty arises in determining the sign of the rotation angle. To eliminate this uncertainty, two probing lasers with different wavelengths can be used (inset in Fig. 2).

Numerical simulations were carried out using a transfer matrix [16]. In this method the field amplitudes at the input (E_{j-1}) and yield (E_j) of the layers boundaries are generally described by the following matrices:

$$\begin{bmatrix} E^t_{(j-1)-} \\ E^r_{(j-1)-} \end{bmatrix} = M_j \begin{bmatrix} E^r_{j-} \\ E^t_{j-} \end{bmatrix} \tag{1}$$

$$M_j = \begin{bmatrix} \dfrac{\exp(i\theta_j)}{g_{j-1}} & \dfrac{f_{j-1}}{g_{j-1}}\exp(-i\theta_j) \\ \dfrac{f_{j-1}}{g_{j-1}}\exp(i\theta_j) & \dfrac{\exp(-i\theta_j)}{g_{j-1}} \end{bmatrix}. \tag{2}$$

Here the index „„–“ corresponds to the reflected wave, t and r correspond to the transverse and radial components of the wave, f and g — Fresnel coefficients:

$$f_{j-1} = \frac{n_{j-1} - n_j}{n_{j-1} + n_j}, \quad g_{j-1} = \frac{2n_{j-1}}{n_{j-1} + n_j}. \tag{3}$$

The transfer matrix is defined by the following expression

$$M = \prod_{j=1}^{m-1} M_j, \tag{4}$$

where m — the number of layers.

The simulation used the dispersion of the optical constants of Si and SiO $_2$ from [17]. Absorption in the photonic crystal was not taken into account. For incident angles less than 15°, the calculation results do not depend on the polarization of the impinging radiation. Therefore, below there are the results only for TM radiation polarization. Mathcad 15 was used in the numerical simulation.

Results and discussion

Figure 3 shows the photonic band gap of a photonic crystal with a defect with optical thickness of layers $\lambda/4$ for different angles of radiation incidence. The width of the band gap for $\theta = 0°$ is $1.35\,\mu$m. The width of the defect guidance band at half maximum is 30 nm. Increasing the thickness of the defect leads to a long-wavelength shift of the defect guidance band and a decrease in the band gap. It can be seen from the figure that a decrease in the band gap affects mainly the spectral shift of the long-wavelength part of the band gap. This effect also affects the spectral shift of the defect guidance band.

Figure 4 (curve *1*) shows the effect of the incident angle on the spectral position of the maximum of the defect guidance band. It can be seen from the figure that the steepness of the dependence increases with increasing incident angle. The average sensitivity to changes in the

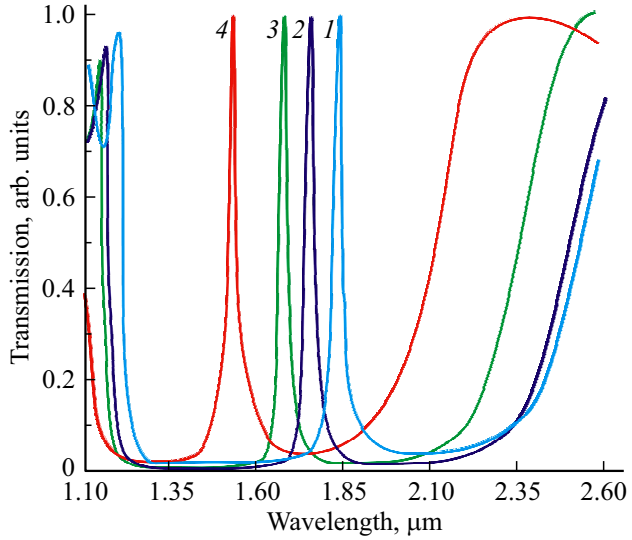

Figure 3. Dependence of the spectral position of the defect guidance band on the angle of incidence of radiation.$\theta = 0°$ (*1*), 5° (*2*), 10° (*3*), 15° (*4*). Optical layer thickness — $\lambda/4$.

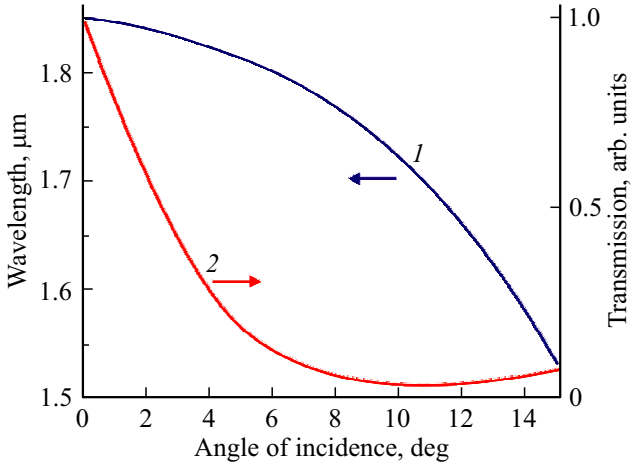

Figure 4. Dependence of the spectral position of the maximum defect guidance band (*1*) and transmittance (*2*) on the radiation incident angle for a fixed wavelength. Optical layer thickness $\lambda/4$.

incident angle for a photonic crystal with this geometry is 20 nm/deg for the angle range $0 < \theta < 15°$.

Figure 4 (curve *2*) shows the effect of the incident angle on the transmittance of a photonic crystal at a fixed wavelength of radiation. This wavelength corresponds to the maximum defect bandwidth for $\theta = 0°$. It can be seen the figure that the maximum slope of the dependence corresponds to the range of incident angles $0 < \theta < 9°$. For a given range of angles, the dependence is close to linear. The sensitivity of transmittance to changes in the incident angle for the $0 < \theta < 5°$ angle range for a fixed wavelength is 1.7 dB/deg. For $\theta > 12°$ there is a slight increase in transmittance. It is caused by a spectral shift of the long-wavelength edge of the photonic band gap to the measurement wavelength.

Let us review the influence of the thickness of photonic crystal layers on its spectral characteristics and sensitivity. Figure 5 shows the photonic band gap of a photonic crystal with a defect for the optical thickness of the layers $10\lambda/4$, the thickness of the defect layer 7 μm and the incident angle $\theta = 0°$. It can be seen from the figure that the photonic band gap is equal to 0.089 μm. The width of the defect guidance band is 4 nm.

Figure 6 (curve *1*) shows the effect of the incident angle on the spectral position of the maximum of the defect guidance band. It can be seen from the figure that the steepness of the dependence increases with increasing incident angle. The average sensitivity to changes in the incident angle for a photonic crystal with this geometry is 6 nm/deg for the angle range $0 < \theta < 6°$. There is maximum steepness of the dependence in the angle range

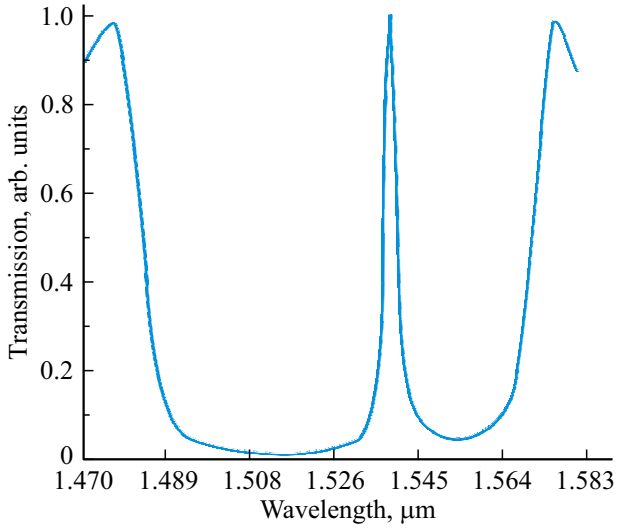

Figure 5. Spectral position of the defect guidance band for the incident angle 0° (optical layer thickness $10\lambda/4$).

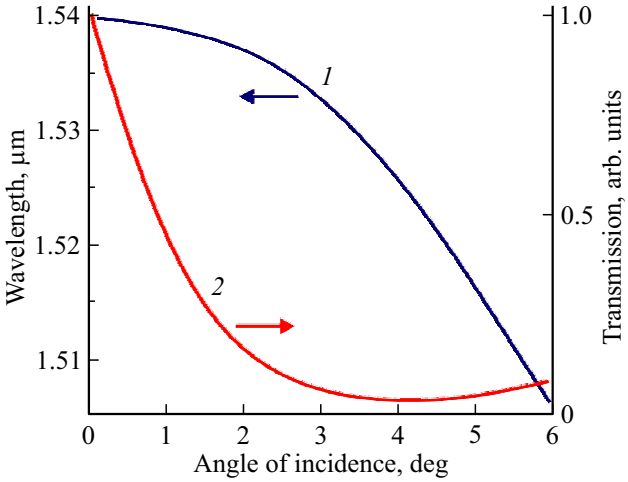

Figure 6. Dependences of the spectral position of the maximum defect guidance band (*1*) and transmittance (*2*) on the radiation incident angle. Optical layer thickness $10\lambda/4$.

Comparison of optical properties and average sensitivity for two 1D photonic crystal geometries

Layer thickness and defect, μm	Photon width band gap, μm	Defect width, nm	Sensitivity nm/deg, angle range	Sensitivity dB/deg, angle range
$\lambda/4$; 0.7 μm	1.35	30	20; $0 < \theta < 15$	1.7; $0 < \theta < 5$
$10\lambda/4$; 7 μm	0.089	4	6; $0 < \theta < 6$	5.5; $0 < \theta < 1.5$

$0 < \theta < 1.6^\circ$. The relationship is approximately linear for this range of angles. The sensitivity of transmittance to changes in the incident angle for a fixed wavelength in the range of incident angles $0 < \theta < 1.6^\circ$ is 5.5 dB/deg (Fig. 6, curve *2*).

Comparison of optical properties and average sensitivity for two 1D photonic crystal geometries with defect is shown in the table. It can be seen the table that an increase in the optical thickness of the layers leads to a decrease in the spectral width of the photonic band gap, the width defect transmittance band, and the range of measurement angles. The maximum sensitivity for measuring angles for the first measurement method has a photonic crystal with layer thickness $\lambda/4$. The maximum sensitivity for measuring angles for the second measurement method has a photonic crystal with layer thickness $10\lambda/4$. In the latter case, the angle 0.07° can be measured, which is close to the sensitivity of a graphene-based angle [18] sensor and a 2D photonic crystal-based angle sensor [15].

Conclusion

Numerical simulation of the optical properties of a 1D photonic crystal with a defect, consisting of layers of silicon and silicon oxide, showed that such a photonic crystal can be used as a rotation angle sensor. The effect is based on the spectral shift of the defect transmittance band as the incident angle changes. The maximum sensitivity when measuring the spectral shift is 20 nm/deg for a photonic crystal with an optical layer thickness of $\lambda/4$. The maximum sensitivity when measuring at a fixed wavelength is 5.5 dB/deg for a photonic crystal with optical layer thickness $10\lambda/4$. The sensor can operate in both transmittance and reflection modes. The sensing element can be located at a distance from the measuring part of the sensor.

Funding

This study was performed as part of the Program „Priority 2030“.

Conflict of interest

The authors declare that they have no conflict of interest.

References

[1] A.S.A. Kumar, B. George, S.C. Mukhopadhyay. IEEE Sens. J. **21**, 7195 (2021). DOI: 10.1109/JSEN.2020.3045461
[2] A.H. Falkne. IEEE Trans. Instrum. Meas. **43**, 939 (1994).
[3] E.B. Mohammed, M. Rehman. IEE Proc.−Sci., Meas. Technol., **150**, 15−18 (2003).
[4] B.P. Reddy, A. Murali, G. Shaga. in Proc. 2nd Int. Conf. Frontiers Sensors Technol. (ICFST), Shenzhen, China, 14 (2017).
[5] C. Schott, R. Racz, S. Huber. Sens. Actuators A, Phys. **132**, 165 (2006).
[6] M. Shan, R. Min, Z. Zhong, Y. Wang, Y. Zhang. Opt. Laser Technol. **68**, 124 (2015). DOI: 10.1007/s12647-020-00410-4
[7] D. Sagrario, P. Mead. Appl. Opt., **37**, 6748 (1998). DOI: 10.1364/AO.37.006748
[8] J.B. Markowski. ES 530B: Res. Proj., Hindawi Publ. Corp. 17 (2008).
[9] A.M.R. Pinto, M. Lopez-Amo. J. Sens., **2012**, 598178 (2012). DOI: 10.1155/2012/598178
[10] S. Upadhyay, V.L. Kalyan. Intern. J. Eng. Res. Techn., **4**, 1006 (2015). DOI: 10.1007/s11468-019-00934-9
[11] Z. Baraket, J. Zaghdoudi, M. Kanzari. Opt. Mater. **64**, 147 (2017). DOI: 10.1016/J.OPTMAT.2016.12.005
[12] A.I. Sidorov, L.A. Ignatieva. Optik **245**, 167685 (2021). DOI: 10.1016/j.ijleo.2021.
[13] E. Chow, A. Grot, L.W. Mirkarimi, M. Sigalas, G. Girolami. Opt. Lett., **29**, 1093 (2004). DOI: 10.1364/OL.29.001093
[14] W.C.L. Hopman, P. Pottier, D. Yudistira, J. van Lith, P.V. Lambeck, R.M. de la Rue, A. Driessen, H.J.W.M. Hoekstra, R.M. de Ridder. IEEE J. Sel. Top. Quant. Electron., **11**, 11 (2005). DOI: 10.1109/JSTQE.2004.841693
[15] B. Neil, X. Chen, J. McCann, C. Blair, J. Li, C. Zhao, D. Blair. Opt. Expr., **29**, 15413 (2021). DOI: 10.1364/OE.425433
[16] M. Born, E. Wolf, Principles of optics: electromagnetic theory of propagation, interference and diffraction of light (Cambridge University, 2000).
[17] E.D. Palik. Handbook of optical constants of solids. V. 3 (San Diego: Academic Press. 1998).
[18] Y. Chen, Y. Fan, Z. Zhang, Z. Zhu, K. Liu, J. Zhang, W. Xu, C. Guo. Opt. Expr. **29**, 41206 (2021). DOI: 10.1364/OE.443842

Translated by E.Potapova